

LREE–Nb mineralization in the south western part of Ambadongar carbonatite complex, Chhota Udepur district, Gujarat, India

The Ambadongar sub-volcanic carbonatite alkali complex is located about 140 km east of Vadodara, Chhota Udepur district, Gujarat, India and falls in Survey of India Toposheet No. 46 K/1. The complex intrudes Bagh sandstone (Cretaceous) and overlying Deccan basalts (Eocene) and is situated in the Narmada rift zone¹. The carbonatites came into prominence in the early 1960s with significant discoveries of fluorite and conspicuous radioactivity located near Chhota Udepur, at Ambadongar, the erstwhile Baroda district, Gujarat². Earlier workers have clarified many aspects of the carbonatite complex^{2,3}.

The Ambadongar carbonatite complex is an example of sub-volcanic diatreme with a ring dyke of sövite which collars the inner rim of carbonatite breccia. Regionally, the area comprises Precambrian granite gneisses, Bagh bed sediments, flows of Deccan traps and carbonatites. The basement rocks are the Precambrian granite gneisses, which are exposed at a distance of about 40 km north of Ambadongar near Chhota Udepur⁴. Later, Bagh sediments were deposited during the Cretaceous period. These were overlain by basaltic flows during the Deccan volcanic activity. The Bagh beds are represented by basal conglomerates overlain by marl, gritty sandstone and fine-grained limestone.

The majority of sedimentary formations record southerly dips of 10°–15°. Reversal of dips is noticed in sandstone and overlying basalts due to doming of sandstone basalt sequence in consequence of forceful injection of carbonatite alkali magma. The effects of doming are noticed around Ambadongar. The sövite forms a large ring-dike (nearly 1.5 km dia.) surrounding an incomplete ring of carbonatite breccia in Ambadongar. Plugs of ankeritic carbonatite intrude the sövite. The ankeritic carbonatite, younger in the carbonatite sequence, forms plugs intrusive into sövite. The central depression of the complex is occupied by the basalts. Sövite, ankeritic carbonatite, carbonatite breccias, etc. are found mineralized with respect to REE, Nb and Th.

Carbonatite breccia can be seen abundantly in the area. The fragments in the

breccia are rounded to sub-rounded, and commonly consist of basement gneisses, sandstone, basalt, alkaline rocks and sövite. The size of the fragments varies from a few cms to more than 10 cm. The matrix is invariably calcitic and at places feldspathic.

Sövite is generally coarse-grained, but often shows large variation in grain size. Coarse-grained sövite is exposed in the inner part of the ring, while fine-grained on its outer margin, and nearer to contact with Bagh sandstone in some areas.

Ankeritic carbonatite occurs in three phases. The first phase consists of thin dykes cutting sövite, the second phase forms large plugs and the third phase consists of thin (2–3 cm) veins. These phases are essentially composed of iron-rich carbonate minerals such as siderite and ankerite. Sideritic carbonatites occur

as thin veins and run only for short distances⁵.

The end of carbonatite activity is marked by the formation of a hydrothermal fluorite deposit in carbonatites and along carbonatite–sandstone contact, but mainly in the sövite⁴. It is pertinent to mention here that the late-stage, silica-rich, barite–fluorite carbonatites of primary phase at Ambadongar host one of the richest fluorite deposits in the world with 11.6 million tonnes of ore reserves, averaging 30% CaF₂, as estimated by the Geological Survey of India⁴. Figure 1 shows the Geological map of Ambadongar area⁶.

REE mineralization is hydrothermal in the Ambadongar carbonatite complex. There are two important ways for the formation of hydrothermal minerals at Ambadongar. (1) Re-equilibration and

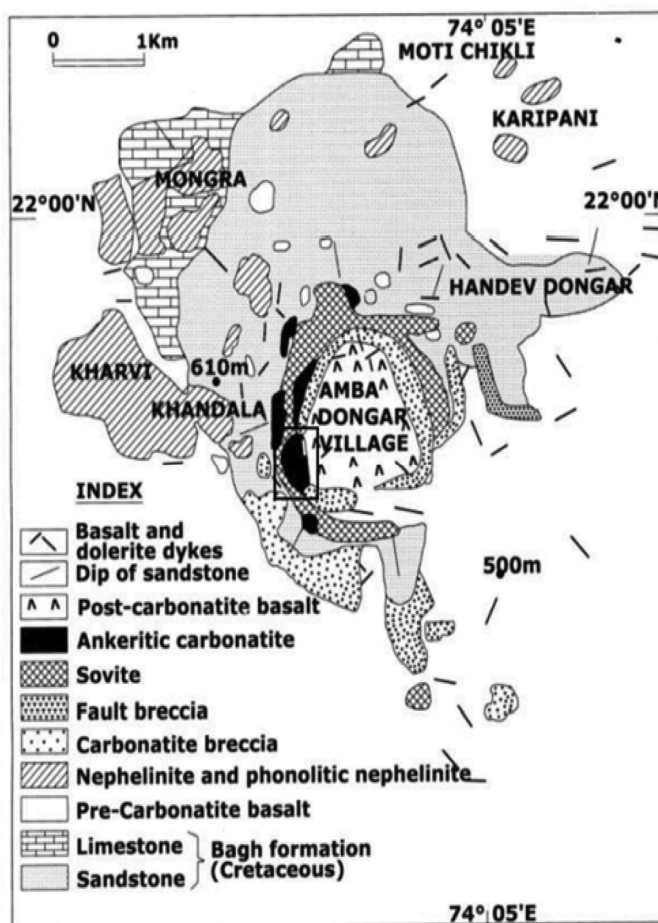


Figure 1. Geological map of the Ambadongar area.

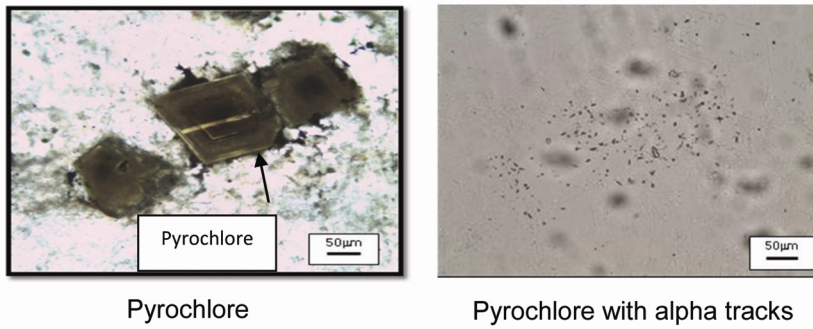


Figure 2. Photomicrographs of carbonatite showing pyrochlore.

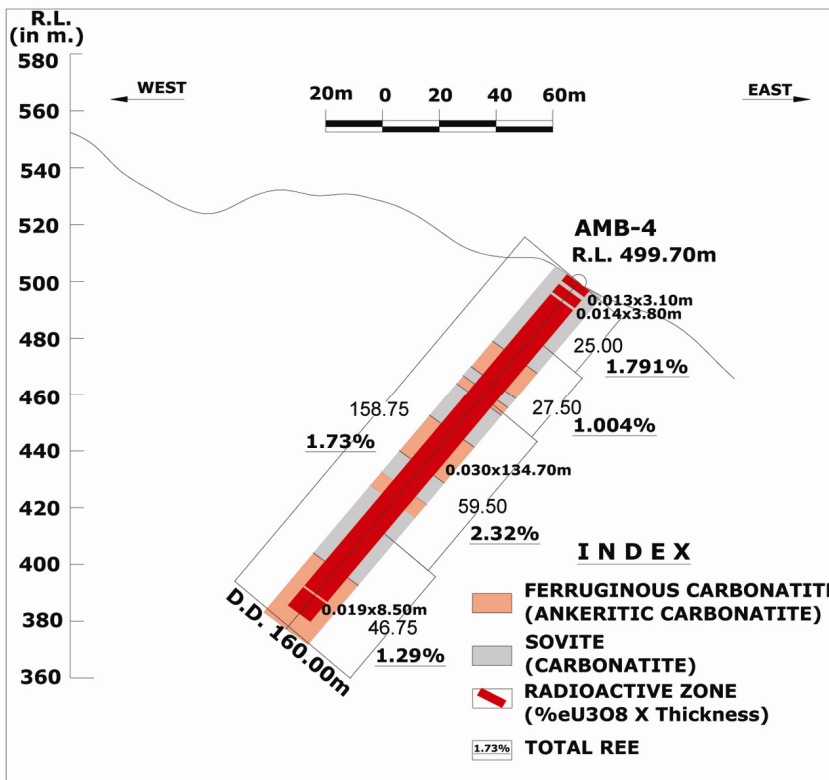


Figure 3. Transverse section of bore hole AMB-4, showing total REE values and radioactive intercepts.

recrystallization of the primary (early crystallized) minerals such as apatite, calcite and pyrochlore, releasing elements to form secondary minerals like strontianite, florencite and columbite. (2) Introduction of key elements from hydrothermal solution into the carbonatites to form quartz, barite, ankerite and REE fluorocarbonates⁶. There is a clear fractionation of REE during crystallization of different phases of carbonatite. Accordingly, REE (LREE) shows increase from earliest alvikite (I) → sövite → alvikite (II) dykes of ankeritic carbo-

natite → plugs of ankeritic carbonatite → sideritic carbonatite⁷. REE abundance in carbonatites, associated silicate rocks and fenites increases in the order fenites < nephelinite < phonolite < pegmatitic sövite < sövites and alvikites < ankeritic carbonatite < ankeritic carbonatite with fluorite, barite and quartz¹.

The ankeritic carbonatites are highly radioactive and show high abundance of REEs, compared to sövite and carbonatite breccia. However, sövites are rich in pyrochlore. Monazite, cerite, thorite and bastnasite are found in ankeritic car-

bonatites⁴. Besides, rare earth fluoro carbonates (bastnasite, synchysite, parasite), florencite, barite, strontianite and columbite are also reported from hydrothermally altered sövite carbonatites⁶. Monazite, bastnaesite, synchysite, florencite and pyrochlore have been identified using XRD method in Atomic Minerals Directorate for Exploration and Research (AMD). Calcite, dolomite and ankerite are the major minerals and other associated minerals like barite, fluorite, quartz, hematite, goethite, epidote, biotite, fluorapatite, rutile and ilmenite have also been identified.

Petro-mineralogical study of core samples recovered from boreholes drilled by AMD resulted in the identification of pyrochlore, which ranges in size from 0.06 to 0.2 mm. It occurs as euhedral grains, yellowish-brown in colour and isotropic. The mineral registered sparse alpha tracks on CN-85 film, indicating its low-order radioactivity. These are translucent, yellow-brown, isotropic, euhedral (often octahedrons) disseminated crystals (Figure 2).

Detailed sampling and a total of 2000 m core drilling were undertaken to understand the subsurface nature of REE mineralization in the southwestern part of Ambadongar ring complex.

In most of the boreholes drilled, the major litho units intercepted were carbonatites (sövite and ankeritic carbonatites) followed by carbonatite breccia. To the best of our knowledge, presence of carbonatite and carbonatite breccia has not been reported earlier below central basalt. The thickness of traps varied from 1.50 to 22.0 m. Subsurface exploration data indicated that carbonatites and carbonatite breccia continued at greater depths and showed significant REE mineralization.

The zone of carbonatite/carbonatite breccia continued below the drilled depth (160 m), indicating possibility of further depth continuation of carbonatite.

Out of 13 boreholes drilled, 6 indicated good mineralization of REE, Nb and Th. A transverse section of one such borehole (AMB/4) showed presence of sövite and ankeritic carbonatite. The average total rare earth elements (TREE) value of the borehole was 1.73% (Figure 3). Mineralization continued till the last drilled depth of 160 m at a vertical impact of around 122 m.

By considering six boreholes over 0.04 sq. km, 140,000 tonnes of total REE

reserves have estimated in 12 million tonnes of ore at an average grade of 1.16% REE with average thickness of 113 m. This includes 136,800 tonnes of REE at an average grade of 1.14% and 3200 tonnes of HREE at an average grade of 0.02%. The explored area is also estimated to contain 10,000 tonnes of Nb₂O₅ at an average grade of 0.08% and 3600 tonnes of Th at an average grade of 0.03%. In addition, the area also shows significant concentration of Ba (average 26,560 ppm), Sr (4960 ppm) and V (467 ppm). These results substantiate the fact that Ambadongar carbonatite complex is a potential target for locating large resources for REE. In addition, Nb, Th and associated elements may be useful by-products. Potential of REE and Nb of Ambadongar area can be compared with the Iron Hill (Powderhorn) carbonatite complex, Colorado, USA⁸.

1. Viladkar, S. G. and Dulski, P., *N. Jb. Miner. Mh. Jg.*, 1986, 37–48.

2. Sukheswala, R. N. and Udas, G. R., *Sci. Cult.*, 1963, **29**, 563–568.
3. Subramaniam, A. P. and Parimoo, M. L., *Nature*, 1963, **198**, 563–564.
4. Viladkar, S. G., In International Carbonatite Workshop, GMDC Science & Research Centre, Ahmedabad, 5–11 December 1996, pp. 1–66.
5. Viladkar, S. G., *Bull. Geol. Soc. Finland*, 1981, 17–28.
6. Doroshkevich, A. G., Viladkar, S. G., Ripp, G. S. and Burtseva, M. V., *Can. Mineral.*, 2009, **47**, 1105–1116.
7. Viladkar, S. G., In *Geochemistry–Earths System Processes* (ed. Panagiotaras, D.), 2012, pp. 485–500.
8. Van Gosen, B. S., Open File Report 2009-1005, U.S. Department of the Interior and US Geological Survey, 2009, pp. 1–27.

ACKNOWLEDGEMENTS. We thank our colleagues in the Chemical Laboratory of the Western Region, Headquarter and Central Region, AMD for quick analysis of a large number of samples and Petrology Laboratory for petrographical studies and XRD Laboratory for REE minerals identification.

Received 22 November 2017; revised accepted 16 February 2018

B. NAGABHUSHANAM^{1,*}
S. DURAI RAJU²
K. L. MUNDRA³
S. D. RAI¹
R. K. PUROHIT¹
M. B. VERMA¹
L. K. NANDA¹

¹Atomic Minerals Directorate for Exploration and Research,

Hyderabad 500 016, India

²Atomic Minerals Directorate for Exploration and Research, Beach Sand and Offshore Investigations, Thiruvananthapuram 695 012, India

³Atomic Minerals Directorate for Exploration and Research, Western Region,

Jaipur 302 033, India

*For correspondence

e-mail: bnagabhushanam.amd@gov.in

Chronic flubendiamide exposure induces oxidative stress in water buffalo (*Bubalus bubalis*) calves

Flubendiamide is a recently introduced, fast-acting insecticide with an excellent residual effect¹. In an unpublished study, it was reported not to cause any genotoxic, carcinogenic and neurotoxic effects in mammals. However, recent studies suggest that it is toxic for fish² and Chinese tiger frog³. Alterations in leukogram⁴, erythrocytic indices⁵ and aspartic acid concentration in cerebrospinal fluid⁶ in water buffalo following its chronic exposure to flubendiamide have also been recorded in our laboratory.

The knowledge about toxicopathology of flubendiamide in mammals is limited at present. Recently, oxidative stress has been reported as an important biomarker of flubendiamide toxicity in soil-dwelling bacteria⁷ and in a freshwater invertebrate, *Daphnia magna*⁸. The present study, therefore, aimed to examine changes in oxidative stress indices in blood of buffalo calves exposed to flubendiamide.

Eight healthy, 8–12-month-old, male water buffalo calves (*Bubalus bubalis*) with body weight between 120 and

180 kg, were provided a balanced ration, dewormed and acclimatized for two weeks at experimental animal shed of the department. The experiment was conducted after approval from the University Animal Ethics Committee. The animals were divided into two equal groups. Group I (healthy control) did not receive any treatment and group II animals received flubendiamide (Fame, Bayer Cropscience Limited, Gujarat) @ 0.024 mg/kg/day orally for 90 consecutive days. Blood samples were collected on 0, 30th, 60th and 90th days of treatment and day-30 post-treatment.

Lipid peroxides (LPO) in erythrocytes, blood glutathione (GSH) concentration, plasma total antioxidant activity (TAA) and activities of superoxide dismutase (SOD), catalase, glutathione peroxidase (GP_x), glutathione reductase, glutathione-S-transferase and glucose-6-phosphate dehydrogenase (G6PD) in erythrocytes were estimated by standard protocols as described elsewhere⁹. The data obtained were analysed by Student's *t*-test and

one-way ANOVA with Turkey's post-hoc test using SPSS 16.0 software package. The significance was assessed at $P < 0.05$.

Flubendiamide exposure resulted in a significant increase in LPO to a level higher than the control group by 29.78% on day-60 and by 49.38% on day-90 (Table 1). LPO level declined on day-30 post-treatment, but it remained significantly higher than control. Blood glutathione level was significantly lower (29.32%) than control on day-90. However, the level on day-30 post-treatment increased to become statistically comparable to control. TAA did not show any significant difference up to day-60, but on day-90 it was significantly lower (24.87%) than control. Post-treatment the value increased on day-30 to become statistically comparable to control.

SOD activity in erythrocytes declined on day-90 to become significantly lower (17.94%) than control. However, activity increased on day-30 post-treatment to become comparable to control (Table 2).